The influence of wavelength on phase transformations induced by picosecond and femtosecond laser pulses in GeSb thin films

S. M. Wiggins, J. Bonse, J. Solis, C. N. Afonso, K. Sokolowski-Tinten et al.

Citation: J. Appl. Phys. **98**, 113518 (2005); doi: 10.1063/1.2139830
View online: http://dx.doi.org/10.1063/1.2139830
View Table of Contents: http://jap.aip.org/resource/1/JAPIAU/v98/i11
Published by the American Institute of Physics.

The influence of wavelength on phase transformations induced by picosecond and femtosecond laser pulses in GeSb thin films

S. M. Wiggins,[a] J. Bonse, J. Solis,[b] and C. N. Afonso
Instituto de Optica, CSIC, Serrano 121, E-28006 Madrid, Spain

K. Sokolowski-Tinten
Institut für Optik und Quantenelektronik, Friedrich-Schiller-Universität Jena, Max-Wien-Platz 1, D-07743 Jena, Germany

V. V. Temnov,[c] P. Zhou, and D. von der Linde
Institut für Experimentelle Physik, Universität Duisburg-Essen, D-45117 Essen, Germany

(Received 6 June 2005; accepted 25 October 2005; published online 12 December 2005)

Cycling between the crystalline and amorphous phases of 25-nm-thick GeSb films induced by single laser pulses of duration of 100 fs or 20 ps is investigated in the 400–800 nm wavelength range. The time evolution of the phase transformations has been studied with picosecond resolution real-time reflectivity measurements at a probe wavelength of 514.5 nm and also with femtosecond and picosecond pump-probe measurements. Upon picosecond irradiation, three regimes are identified: for wavelengths below ~550 nm and above ~750 nm, the total time to transform between the crystalline and amorphous phases is of the order of 10–24 ns while in the intermediate wavelength range of 600–750 nm, the transformation time is only ~650 ps. Upon 100 fs irradiation, the transformation times are observed to decrease with increasing wavelength with the shortest times of ~5 ns for crystallization and ~10 ns for amorphization, both occurring at 800 nm. This behavior is discussed in terms of how the wavelength-dependent refractive index of the phases involved influences the initial supercooling of the molten volume and the subsequent resolidification scenario. © *2005 American Institute of Physics*. [DOI: 10.1063/1.2139830]

I. INTRODUCTION

Laser-induced phase transitions in absorbing materials have been extensively studied over recent years and have been featured in a wealth of applications in materials science.[1] Of particular relevance to this article is the field of phase-change optical data storage where, typically, the different optical properties, i.e., the reflectivity, of the amorphous (a) and crystalline (c) phases of the recording material allow binary data to be encoded.[2] In rewritable systems, each transformation between the two phases is reversible upon irradiation with a single laser pulse of a different fluence. Present commercial phase-change optical recording systems, such as those based on GeSbTe (Ref. 3) or AgInSbTe,[4] use laser pulses of tens of nanosecond duration for write (amorphize) or erase (crystallize) operations.

Since the obvious limiting factor for the transformation time is the pulse duration of the laser itself, over the last years there has been an intense search for faster transforming materials, which has largely concentrated on Sb-based materials such as InSb,[5] GaSb,[5] and GeSb,[5,6] while there have been a number of studies into the phase transformation dynamics of current and potential data storage materials upon picosecond[6–9] and femtosecond[6,7,10–14] laser-pulse excitations. In this context, it is important to consider that the phase switching associated with the write/erase processes involves in many cases rapid melting phenomena. In such a case, a distinction can be made between that induced by a picosecond or nanosecond laser pulse,[15] which is a classical thermal process, and that induced by a femtosecond laser pulse,[16] where electronic excitation can be significant and the transition can therefore be initially nonthermal in nature.[17] Note, however, that even when ultrafast nonthermal melting occurs, the electrons and the lattice reach thermal equilibrium typically within a few picoseconds so that subsequent resolidification of the material on a much longer time scale is still a thermal process.[18]

To date, the shortest reported transformation times in optical recording materials have been those induced by 30 ps pulses at 583 nm in 25-nm-thick Sb-rich GeSb films on glass substrates where the complete $a \leftrightarrow c$ transformation times were as low as ~400 ps.[19] Such rapid phase transformations represent a significant improvement with respect to the current commercial systems. They are achieved via complete melting of a film on a low-thermal-conductivity substrate. This facilitates a very large supercooling in the melt volume which drives a rapid bulk solidification process. In this process the solid phase nucleates at extremely large rates throughout the whole molten volume, initially at homogeneous temperature.[19] In general, Sb-rich GeSb films have great potential for this application because reversible phase changes have been demonstrated upon picosecond and femtosecond irradiations while exhibiting sufficient optical contrast between the a and c phases.[6] Recently, it has been observed that analogous excitation of the same 25-nm-thick

[a]Electronic mail: m.wiggins@phys.strath.ac.uk
[b]Author to whom correspondence should be addressed; electronic mail: j.solis@io.cfmac.csic.es
[c]Present address: Experimentelle Physik IIb, Universität Dortmund, Otto-Hahn-Strasse 4, D-44221 Dortmund, Germany.

film with pulse durations in the range of 100 fs–1.5 ps greatly lengthens the transformation time for amorphization to 10–15 ns.[13] This unusual behavior of an *increased* transformation time upon irradiation with a *shorter* duration pulse has been attributed to the excessive initial supercooling generated by pump pulses with a duration shorter than or close to the electron-phonon relaxation time. Such an excessive supercooling induces a very high initial solid-phase nucleation rate such that the latent solidification heat released is high enough to greatly reduce the supercooling, finally leading to a slowing down of the whole resolidification process,[20] i.e., a phenomenon usually referred to as recalescence.

In this article we build on these initial results obtained with a pump wavelength ~600 nm with an investigation of the $a \leftrightarrow c$ transformations induced by both 20 ps and 100 fs laser pulses as a function of wavelengths across the range of 400–800 nm. This has been motivated by the fact that the complex refractive index, which governs the energy absorption profile via the optical penetration depth, is wavelength dependent. The aim of this work is therefore to gain a better understanding of phase transformations induced in GeSb thin films by ultrashort laser pulses with a view towards achieving even shorter transformation times.

II. EXPERIMENTAL METHODS

The samples are 25-nm-thick $Ge_{0.07}Sb_{0.93}$ films grown by dc magnetron sputtering on 1-mm-thick glass substrates. In order to investigate the structural transformation dynamics of the films under laser excitation, the time evolution of the surface reflectivity of the samples has been measured using three different experimental setups with either 100 fs or 20 ps irradiation pulses.

In each configuration, a Ti:sapphire regenerative amplifier supplying pulses with a duration of ~100 fs at a wavelength of 800 nm has been used either to irradiate the samples or to produce pulses with different durations and/or wavelengths. Second-harmonic generation in a beta-barium borate (BBO) crystal enabled 400 nm femtosecond pulses to be generated, while femtosecond pulses at all intermediate wavelength pulses have been produced in an optical parametric amplifier (OPA) pumped by the Ti:sapphire amplifier. Pulses of 20 ps duration have been obtained either by control of the compressor elements in the Ti:sapphire amplifier itself or by external stretching of the frequency-doubled amplifier pulses or OPA-generated pulses via a double pass through a diffraction grating pair.[21]

The as-grown, amorphous films have been locally crystallized beforehand at each particular wavelength by a series of low-fluence (~15 mJ/cm^2) pulses. The *c*-to-*a* phase transformation has then been induced by single laser pulses at higher fluences (40–60 mJ/cm^2). Subsequent recrystallization of the same area can be achieved by further single-pulse irradiation at lower fluences (15–20 mJ/cm^2). Over each of these narrow ranges, the precise value of the fluence has little effect on the total transformation time.[13]

The first experimental setup comprises real-time reflectivity (RTR) measurements that have been carried out using externally modulated 1 μs pulses from a single-mode

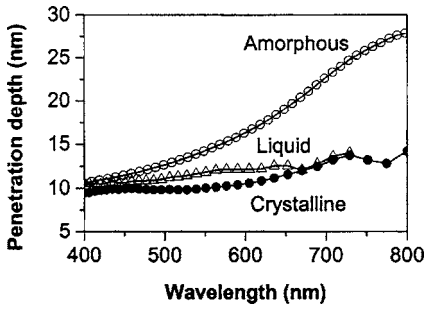

FIG. 1. Dependence of the optical penetration depth (normal incidence) on the pump wavelength for the crystalline, liquid, and amorphous phases of bulk GeSb based on dielectric function data from Ref. 25.

Ar^+-ion laser (used as the probe beam) operating at 514.5 nm. These pulses are incident at 19° to the sample and are focused onto the center of the irradiated region that has been excited by the normally incident pump pulse with a wavelength between 400 and 800 nm. The probe reflectivity has been simultaneously recorded by a fast photodetector coupled to a sampling oscilloscope and by a streak camera.[22] The temporal resolutions of the two detection systems are in the nanosecond and picosecond time scales, respectively. To account for the relatively low signal-to-noise ratio in the captured streak camera transients, many reflectivity transients are taken for each experimental configuration so that a mean transformation time can be determined.

Secondly, a conventional picosecond pump-probe (ps-PP) system has been used at a wavelength of 600 nm with a 20 ps pump pulse focused onto the film surface at normal incidence and a 20 ps probe pulse focused onto the center of the irradiated region at an angle of 12°. The intensity of the reflected probe signal has been measured by a photodiode coupled to an oscilloscope. At each probe delay, an average over several shots in fresh regions of the sample is obtained in order to compensate for the shot-to-shot fluctuations that are present. The temporal resolution of the pump-probe experiment is limited by the duration of the probe pulse itself and is 20 ps in this case. Further details of this experimental setup are given in Ref. 23.

Lastly, additional pump probing has been conducted using the femtosecond time-resolved microscopy (fs-TRM) technique.[18,24] In this setup, images of the surface are captured on a digital camera upon illumination with a 400 nm wavelength and a 100 fs duration probe pulse. The pump pulse (picosecond or femtosecond duration) is incident at an angle of 45°, and the pump wavelength has been set as either 400 or 800 nm. The temporal resolution of this setup is close to the 100 fs duration of the probe pulse.

III. RESULTS AND DISCUSSION

In order to provide an initial description of how the wavelength of the pump pulse can affect the material transformation dynamics upon laser exposure, Fig. 1 shows the corresponding optical penetration depths for the crystalline (*c*), amorphous (*a*), and liquid (*l*) phases of GeSb across the wavelength interval of interest. The complex refractive indices corresponding to the *a* and *c* phases over the 400–800 nm interval have been determined by spectroscopic el-

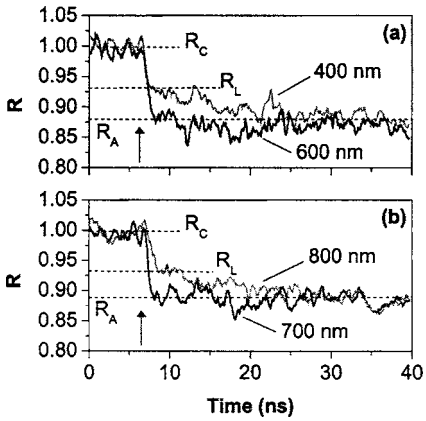

FIG. 2. Normalized streak camera reflectivity transients on crystalline GeSb induced by single 20 ps pump pulses of wavelengths (a) 400 and 600 nm and (b) 700 and 800 nm (RTR setup with a 514.5 nm probe pulse). Each arrow indicates the arrival time of the pump pulse to the surface. R_C, R_A, and R_L denote the reflectivities corresponding to the crystalline, amorphous, and liquid phases.

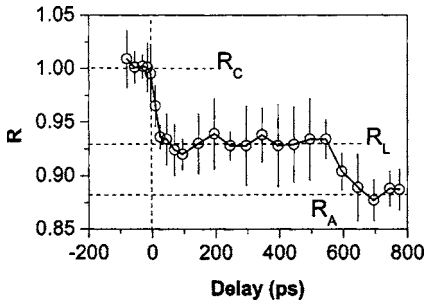

FIG. 3. Normalized reflectivity change on crystalline GeSb as a function of probe delay for irradiation by a single 20 ps, 600 nm pump pulse (ps-PP setup with 600 nm, 20 ps probe pulse). The vertical dashed line indicates the arrival of the pump pulse to the surface.

lipsometry. The values corresponding to the liquid phase have been determined by femtosecond time-resolved measurements of the evolution of the dielectric function upon irradiation with 100 fs pulses using a white-light probe generated with an 800 nm pulse. They are therefore limited to a wavelength interval of approximately 400–750 nm.[25]

The optical penetration depth is given by $d=\lambda/(4\pi k)$ where λ is the wavelength and k is the imaginary part of the complex refractive index. The uncertainty in the value of d is essentially given by that associated with the value of the imaginary part of the refractive index k. The error in the determination of k is typically below 5% in the case of spectroscopic ellipsometry measurements (a and c phases) or about 5% for the femtosecond time-resolved measurements of the evolution of the dielectric function (l phase). The larger uncertainty in this latter case is related to the uncertainties in the single-pulse exposure reflectivity measurements at different angles from which the dielectric function is determined.[26]

In general terms, the penetration depth of each of the GeSb phases increases with increasing wavelength, with the curves for l-GeSb and c-GeSb showing a somewhat smoother behavior most likely related to their semimetallic nature. The optical properties of the molten phase will be particularly relevant when we consider the effect of irradiation with 20 ps laser pulses since melting can be induced in this case over a time shorter than the pulse duration, causing the pulse to partly interact with the molten material.

A. Picosecond pulse irradiation

Figure 2 depicts the entire wavelength interval of interest with RTR streak camera transients (50 ns time window) showing the time evolution of the reflectivity during the c-to-a transformation. For this streak camera time window, the nominal time resolution of the detection system is about 350 ps. The probe intensity signal has been normalized to the initial reflectivity level of the crystalline phase R_C, and the transformation time is defined as the time that elapsed from the arrival of the pump pulse until the final state reflectivity is reached. The dashed horizontal line marked R_L indicates the theoretical reflectivity of the liquid phase as calculated by a thin-film optical model applying the refractive indices [c-GeSb $(n+ik)$ (515 nm)$=2.08+i4.18$, l-GeSb $(n+ik)$ (515 nm)$=2.00+i3.62$].[25] In each transient of Fig. 2, the reflectivity is seen to decrease rapidly after the arrival of the pump pulse with the solid-to-liquid melt-in times convoluted by the nominal time resolution of the detection system. Note that the relatively long melt-in time shown for the 800 nm pump [Fig. 2(b)] arises from the low signal-to-noise ratio inherent to the streak camera transients.

At pump wavelengths of 400 nm [Fig. 2(a)] and 800 nm [Fig. 2(b)], the reflectivity remains around that of the liquid state for several nanoseconds before decreasing slowly to that corresponding to the final amorphous phase R_A. For the wavelengths 400 and 800 nm, a slow total transformation time of the order of 12–15 ns has been observed. By contrast, at pump wavelengths of 600 nm [Fig. 2(a)] and 700 nm [Fig. 2(b)], the reflectivity falls directly to that of the amorphous phase over a time of the order of the temporal resolution of the experiment, indicating that fast (subnanosecond) c-to-a transformations have been induced.

The total optical contrast between the a and c phases of 12% is slightly less than the 14% predicted from the refractive index [a-GeSb $(n+ik)$ (515 nm)$=3.15+i3.13$][25] but equal to that obtained in steady-state measurements. The slight decrease from the optimal value is due to the low pump-to-probe size ratio achievable after stretching and tight focusing of the pump pulse.

Observation of a subnanosecond transformation time has previously been reported using the single-shot RTR streak camera experimental setup described above for irradiation with picosecond pulses at wavelengths around 600 nm.[13,19] As shown in Fig. 3, these results have been further confirmed here and improved in terms of time resolution. The latter shows the time evolution of the reflectivity for the c-to-a transformation as determined with the ps-PP setup. Each error bar in the data represents the standard deviation after averaging over several shots. Upon irradiation with a 20 ps pump pulse at 600 nm of mean fluence $\sim 50\ \mathrm{mJ/cm^2}$, the reflectivity decreases in some tens of picoseconds (the time resolution in this case is given by the 20 ps pulse duration of the probe), indicating the formation of an optically thick liquid layer with reflectivity R_L. The good agreement between

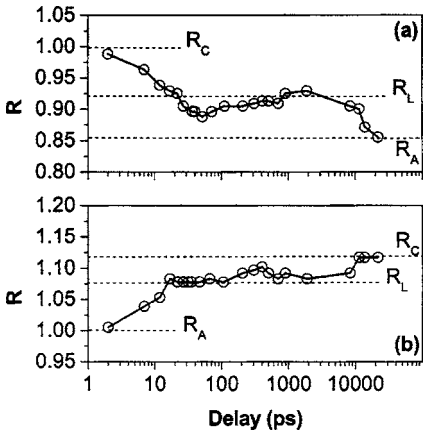

FIG. 4. Normalized reflectivity change on (a) crystalline and (b) amorphous GeSb as a function of probe delay for irradiation by a single 20 ps, 800 nm pump pulse (fs-TRM setup with 400 nm, 100 fs probe pulse).

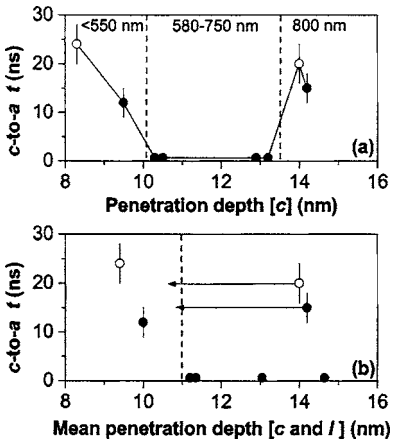

FIG. 5. Dependence of the *c*-to-*a* transformation time *t* for a pump pulse duration of 20 ps on the optical penetration depth *d* normal to the surface of (a) the crystalline phase only and on (b) the mean of the crystalline and liquid phases. Open points denote fs-TRM measurements and closed points denote RTR measurements. The vertical dashed lines indicate the approximate threshold values for obtaining a fast transformation time in the subnanosecond range. The horizontal arrows on the 800 nm data points show the effect of a reduced optical penetration depth into liquid.

the experimental and calculated reflectivity levels of the liquid phase indicates the presence of liquid GeSb for delays up to 550 ps. The reflectivity is then seen to decrease again, reaching the corresponding value of the amorphous phase R_A within ~100 ps.

The *c*-to-*a* transformation time of ~650 ps evident from Fig. 3 is consistent with the values of ~400 ps reported previously[13,19] and is more accurate given the better time resolution achieved with the pp-PP setup. More significantly, the *liquid-to-amorphous* transition time is clearly resolved to occur within ~100 ps (Fig. 3). This allows an estimation of the solid-phase nucleation rate upon bulk solidification to be made. Assuming spherical nuclei with diameters equal to the film thickness resulting from separate nucleation events[27] and using the observed solidification time, a nucleation rate of $\sim 1 \times 10^{33}$ events/(m^3 s) for the re-amorphization process is obtained. For the reverse *a*-to-*c* transition that has previously been observed to occur on a subnanosecond time scale as well,[19] a similar nucleation rate would be deduced. These values provide a clear indication of the extremely fast solidification process that takes place under picosecond pulses in the 550–750 nm interval.

Further pump-probe measurements have been conducted with the fs-TRM setup for wavelengths below 550 nm and above 750 nm, providing results consistent with those shown in Fig. 2 which have been measured with the streak camera RTR setup. Figure 4 shows the time evolution of the probe reflectivity for both the *c*-to-*a* and *a*-to-*c* transformations upon irradiation with a 20 ps pump pulse at an 800 nm wavelength. Typical examples of the recorded images in thicker samples have been presented elsewhere.[28] Although in this case the pump pulse angle of incidence is 45°, the large value of the real part of the complex refractive index for each solid phase means that the angle of refraction is only 10° in each case. The optical penetration depth normal to the surface is therefore reduced by only 2%.

In the laser-induced amorphization process shown in Fig. 4(a), melting is seen to occur in around 10 ps. This melt-in time is somewhat shorter than the one previously measured in the ps-PP experiment at 600 nm (Fig. 3) due to the improved temporal resolution associated with the use of 100 fs probe pulses. Moreover, it is known that the reflectivity of a liquid phase can decrease after rapid melting due to the temperature dependence of the complex refractive index[29,30] of the molten phase. The high spatial resolution (few micrometers) of the fs-TRM setup enables this phenomenon to be resolved here such that the observed reflectivity level of the liquid phase drops initially below that of the theoretical liquid level R_L. The drop of ~3% agrees well with that predicted from dielectric function data[25] acquired for a hot liquid some tens of picoseconds after the femtosecond-pulse-induced melting of a GeSb film. The reflectivity finally reaches R_L at ~1 ns and solidification proceeds slowly from ~2 ns until the final amorphous reflectivity is reached after ~20 ns. An even longer transformation time of ~24 ns has been obtained for irradiation with a 400 nm pump pulse (not shown). The recrystallization shown in Fig. 4(b) also evidences a slow resolidification process with the transformation time being ~10 ns. The small transient peak in reflectivity at ~400 ps may indicate a partial remelting of the film upon the initial solid-phase nucleation. For both processes, amorphization and crystallization, the transformation time is well above the subnanosecond time observed intermediate irradiation wavelengths (550–750 nm).

Three regimes under picosecond irradiation can therefore be identified, as shown in Fig. 5(a) which depicts the *c*-to-*a* transformation time as a function of the effective penetration depth of the pump pulse into the initially crystalline material. Given the accuracy of the wavelength and refractive index measurements for the different GeSb phases (see description of Fig. 1 above), the effective optical penetration depth can be calculated with an absolute accuracy better than 0.5 nm. The optimal transformation behavior is in the central regime between ~550 and 750 nm where the lowest transformation times between ~400 and 700 ps have been observed. The values plotted in the figure have been measured by the streak camera using a shorter time window (10 ns)

with a better temporal resolution (~100 ps). In this optimal wavelength range, the energy deposition conditions lead to an initial supercooling in the melt that favors a bulk solidification process but with a nucleation rate not high enough to generate substantial recalescence effects. Decreasing the wavelength, i.e., the optical penetration depth, vastly increases the transformation time, and this defines the left-hand regime (below ~550 nm) where more energy is absorbed in a shallower depth of the film driving a greater initial supercooling and nucleation rate. Under these conditions, the rate of latent heat release is sufficient to reduce the supercooling greatly, retarding globally the solidification process and lengthening greatly the transformation time; i.e., recalescence effects are significant.

The right-hand regime of Fig. 5(a), which consists of irradiation at 800 nm, appears to be somewhat anomalous given that the greater penetration depth into the crystalline phase would lead to recalescence effects being even less significant than in the central regime. To resolve this, it must be considered that under picosecond pulses, melting can be induced during the absorption of the irradiation pulse, causing the pulse to partly interact with the already molten material. As shown in Fig. 4(a), melting occurs after ~10 ps. It is reasonable, therefore, to make the crude approximation that for the 20 ps pulses used, the leading half of the pump pulse interacts with the initially solid phase and the trailing half with the newly molten material. The transformation times can then be plotted as a function of the mean value of the crystalline and liquid penetration depths, as shown in Fig. 5(b). The behavior for irradiation at 800 nm then needs qualifying because, unfortunately, it is not possible to place these two data points (corresponding to normal-incidence RTR and 45° incidence fs-TRM measurements at 800 nm) directly into the scheme of Fig. 5(b). The reason for this is the absence of reliable data for the refractive index of the liquid phase at this wavelength (800 nm was the wavelength used to generate the white-light probe applied in the time-resolved dielectric function measurements of Ref. 25). Clearly, however, the interaction with the liquid phase will have one of two possible consequences depending on the value of the penetration depth into the liquid.

First, an increased optical penetration depth into the liquid, akin to that of the crystalline phase or even larger, would just render the behavior to be equally anomalous since energy absorption in a greater depth drives a smaller initial supercooling and nucleation rate upon bulk solidification. Recalescence effects should be as negligible as in the 550–750 nm region, and a fast transformation time would therefore be expected. This has clearly not been observed. Also, alternative scenarios involving a slow interfacial solidification process to account for the long transformation times have been eliminated by performing time-resolved reflectivity measurements at the film/substrate interface that confirm a predominantly bulk solidification process. A high value for the penetration depth into the liquid therefore seems unlikely.

Conversely, a slightly decreased optical penetration depth into the liquid at 800 nm would allow the behavior at this point to be understood in the same framework as for wavelengths below ~500 nm, with increased supercooling being preceded by energy absorption in a shallower depth of the material. To be consistent with the scheme of Fig. 5(b), a penetration depth into the liquid of ~8 nm would be required. The 800 nm fs-TRM measurement of Fig. 4(a) which showed a very slow transformation time of ~20 ns is also more consistent with that of Fig. 5(b) when such a decreased optical penetration depth into the liquid phase is applied. In this way, a threshold between fast and slow transformations under picosecond pulses is seen to occur at an average solid-liquid mean penetration depth of ~11 nm. This corresponds to normal-incidence irradiation at ~550 nm, thus defining the upper wavelength limit of the left-hand regime of Fig. 5(a).

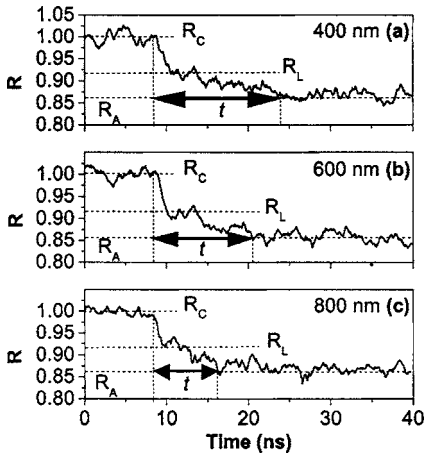

FIG. 6. Normalized streak camera reflectivity transients on crystalline GeSb induced by single 100 fs pump pulses of wavelengths (a) 400, (b) 600, and (c) 800 nm where t indicates the transformation time (RTR setup with 514.5 nm probe pulse).

Thus it is proposed that for 20 ps irradiation across the entire wavelength interval, the solidification proceeds via a bulk process and when the supercooling is not above some threshold, i.e., for a wavelength ~550–750 nm, recalescence effects do not manifest themselves and the solidification occurs rapidly within several hundreds of picoseconds. When the penetration depth into the initial solid phase and/or the liquid phase is sufficiently small, i.e., for wavelengths below ~550 nm and at ~800 nm, supercooling is increased to such an extent that recalescence effects drastically retard the solidification.

B. Femtosecond pulse irradiation

Analysis of the behavior upon irradiation with pulses of duration ~100 fs is somewhat simplified by the fact that this duration is much shorter than the electron-phonon relaxation time of GeSb. This time has been estimated to be ~800 fs for a-GeSb.[31] We can thus expect the crystalline phase to show a value not that different from those within an order of magnitude. Hence, the femtosecond pump pulse does not interact with the liquid phase of the film, and only the optical penetration depth into the initial solid phase has to be considered.

Figure 6 shows RTR streak camera transients for the c-to-a transformation induced by 100 fs pulses of wavelengths 400 nm (a), 600 nm (b), and 800 nm (c). The optical

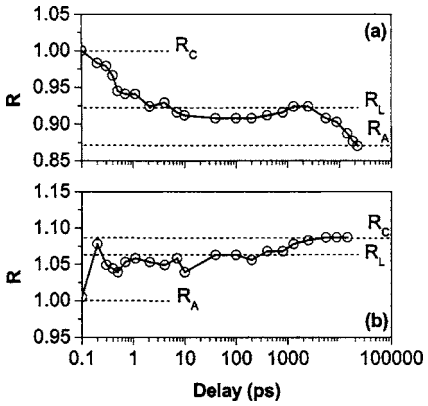

FIG. 7. Normalized reflectivity change on (a) crystalline and (b) amorphous GeSb as a function of probe delay for irradiation by a single 100 fs, 800 nm pump pulse (fs-TRM setup with 400 nm, 100 fs probe pulse).

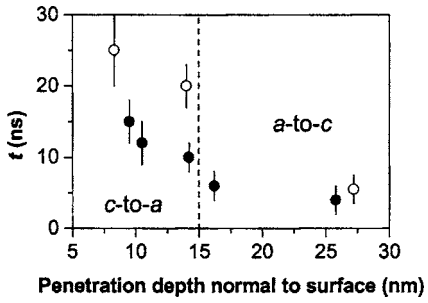

FIG. 8. Dependence of the transformation time t on the pump pulse optical penetration depth normal to the surface for a pulse duration of 100 fs. Open points denote fs-TRM measurements and closed points denote RTR measurements.

contrast is ~14% in each case, thereby agreeing very well with that calculated using the complex refractive index data as discussed earlier. (Under femtosecond pumping, the absence of additional pulse stretching elements has allowed the pump-to-probe size ratio to be improved, with respect to picosecond pumping, and there is no decrease in optical contrast in this case.) There is a smooth dependence of the transformation time on the wavelength, with the time rising from a value of ~10 ns at 800 nm [Fig. 6(c)] to~15 ns at 400 nm [Fig. 6(a)]. Across the entire wavelength interval, therefore, the transformation time is long with respect to the optimal picosecond pulse behavior. Significantly, however, at 800 nm, the femtosecond-pulse-induced transformation time is ~5 ns *shorter* than the corresponding picosecond-pulse-induced time [Fig. 2(b)], thus confirming the role played by the interaction of the latter part of the 20 ps pump pulse with the liquid phase. Only at this wavelength is the transformation time shorter for femtosecond pumping, thus supporting the suggestion that the penetration depth into the liquid is reduced at 800 nm.

Figures 7(a) and 7(b) show the corresponding reflectivity evolution under 800 nm, 100 fs pulses obtained with the fs-TRM setup for both *c*-to-*a* and *a*-to-*c* transitions. The overall behavior in Fig. 7(a) is consistent with that shown in Fig. 6(c) and is qualitatively similar to that for picosecond irradiation [Fig. 4(a)], with the main difference being that melting occurs more rapidly, in a few picoseconds, because of the much shorter pulse duration. The liquid reflectivity level is maintained for up to 2 ns before the eventual amorphization at ~20 ns. Within the experimental error, this transformation time is approximately equal to that measured by the same technique for picosecond pumping. The *a*-to-*c* transformation of Fig. 7(b) is characterized by a high reflectivity level on the subpicosecond time scale that may indicate an ultrafast phase transition.[28] The total transformation time of ~5 ns is once again significantly shorter than that of the corresponding picosecond irradiation [Fig. 4(b)].

The femtosecond data are summarized in Fig. 8 which shows the transformation time as a function of the effective penetration depth for both femtosecond-laser-induced amorphization and crystallization. Both transformations display longer times as their respective penetration depths decrease. Note that it is not possible to directly compare the transformation times for the two transformations because the pump fluence is two to three times higher for amorphization. It is also worth noting that, as in the case of picosecond pumping (see Fig. 5), the "long" transformation times measured by fs-TRM are several nanoseconds longer than those measured with the streak camera RTR setup. This arises from the high spatial resolution of the former where averaging of the reflected probe intensity has been conducted over a narrow cross section of the transformed region passing through its center. By contrast, the latter RTR setup averages over the entire Gaussian-shaped probe spot area, including the cooler edges of the transformed region that solidify more rapidly than the warmer center (owing to the Gaussian spatial profile of the pump pulse). Excluding the behavior for pumping at 800 nm as discussed above, the transformation times are longer for femtosecond irradiation as compared with picosecond irradiation. The transformation times also arise from the increased initial supercooling and subsequent enhanced recalescence effects when the pump pulse is close to or shorter than the electron-phonon relaxation time and for which the thermal diffusion length is shorter than the optical penetration depth into the initial solid phase.[13]

IV. CONCLUSIONS

Picosecond-laser-induced phase transformations of 25-nm-thick GeSb films on glass substrates have been fully characterized as a function of wavelength. Subnanosecond *c*-to-*a* transformation times have been observed over the wavelength range 600–750 nm. A picosecond time-resolution pump-probe experiment has accurately determined the *c*-to-*a* transformation time to be ~650 ps at a wavelength of 600 nm. Under these conditions, the liquid-to-amorphous transition time has also been determined to be ~100 ps, driven by a very fast bulk solidification process with an estimated initial nucleation rate of ~1 $\times 10^{33}$ events/(m^3 s). The corresponding nucleation rate of crystallization is expected to be of the same order of magnitude given that the *a*-to-*c* transformation occurs on the same order of magnitude time scale.[19] When recalescence effects are significant, for wavelengths below 550 nm and above 750 nm, the transformation times are as long as ~10 ns for crystallization and ~24 ns for amorphization.

To conclude the picosecond observations, it is seen that the wavelength dependence demonstrates the large sensitivity that exists on the penetration depths which vary by only a few nanometers between one regime and another. This sensitivity arises from the nature of this thin-film system—a film thickness of only 25 nm and a poor heat conducting substrate. Changes of the order of 10% in the energy absorption profile are severely influencing the heat-flow dynamics of the system. Optimization of this system has been achieved by determining that the fastest transformations occur within the 580–750 nm wavelength range (including data of Ref. 19). Thus, the use of picosecond laser pulses in this wavelength range generated from semiconductor lasers or fiber laser sources appear to be very promising with respect to the future application of this technology in the field of optical data storage.

In contrast to picosecond irradiation, upon characterizing the transformation behavior for femtosecond excitation, the fastest transformation times are ~5 ns for crystallization and ~10 ns for amorphization occurring at the longest wavelength investigated (800 nm). It has not been possible, therefore, to induce subnanosecond transformations in this film using 100 fs duration pulses in the visible and nearinfrared spectral region. The reason for this highlights the fundamental difference between nanosecond-pulse-induced transformations (such as those applied in commercial optical data storage systems) and femtosecond-pulse-induced transformations. In the former, additional dielectric layers are employed to impede the conduction of heat out of the irradiated area during the long pulse duration in order to maintain a sufficient cooling rate for amorphization to occur.[2] The femtosecond laser-pulse-excited GeSb system investigated here suffers from the energy deposition being too rapid and there not being enough heat extraction during the short pulse duration and just afterwards. This causes the effects of solidification enthalpy under bulk nucleation to become dominant (recalescence), slowing down globally the solidification process.

It is clear now that inducing faster transformation times under femtosecond irradiation requires a thin-film system with a higher overall thermal conductivity to extract some of the excess solidification heat out of the melt. This may be achieved with a substrate material possessing a thermal conductivity higher than that of glass. The use of special substrates to optimize the overall thermal properties has recently been shown to reduce the transformation times in GeSbTe films irradiated with picosecond pulses.[8] However, given the fact that the skin depth is around half the value of the film thickness, an additional transparent layer on top of the film could effectively conduct enough heat away from the front side of the film, thus helping in reducing the recalescence effects. Another option to prevent recalescence effects from dominating may be to reduce the film thickness (optical simulations show that the optical contrast between the two solid phases could be maintained at acceptable levels upon decreasing the film thickness). This would reduce the absolute quantity of latent heat released upon solidification and also would act to bring the substrate, i.e., the heat sink, closer to the region where most of the energy is directly absorbed. Certainly, it can be concluded that reduction of the transformation times upon femtosecond irradiation will require a more sophisticated thin-film system.

ACKNOWLEDGMENTS

This work has been partially supported by the EU in the frame of the TMR Projects XPOSE (HPRN-CT-2000-00160) and FLASH (MRTN-CT-2003-50364). One of the authors (S.M.W.) acknowledges funding by the same XPOSE project. Another author (J.B.) acknowledges the funding of the CSIC through a contract in the frame of the I3P program (Ref. No. I3P-PC2002), co-funded by the European Social Fund.

[1] D. Bäuerle, *Laser Processing and Chemistry*, 3rd ed. (Springer, Berlin, 2000).
[2] K. Schwartz, *The Physics of Optical Recording* (Springer, Berlin, 1993).
[3] N. Yamada, E. Ohno, N. Akahira, N. Nishiuchi, K. Nagata, and M. Takao, Jpn. J. Appl. Phys., Part 1, Part 1 **26**, 61 (1987).
[4] H. Iwasaki, M. Harigaya, O. Nonoyama, Y. Kageyama, M. Takahashi, K. Yamada, H. Deguchi, and Y. Ide, Jpn. J. Appl. Phys., Part 1 **32**, 5241 (1993).
[5] L. van Pieterson, M. van Schijndel, J. C. N. Rijpers, and M. Kaiser, Appl. Phys. Lett. **83**, 1373 (2003).
[6] J. Solis and C. N. Afonso, Appl. Phys. A **76**, 331 (2003).
[7] M. Watanabe, H. Sun, S. Juodkazis, T. Takahashi, S. Matsuo, Y. Suzuki, J. Nishii, and H. Misawa, Jpn. J. Appl. Phys., Part 2 **37**, L1527 (1998).
[8] J. Siegel, A. Schropp, J. Solis, C. N. Afonso, and M. Wuttig, Appl. Phys. Lett. **84**, 2250 (2004).
[9] C. Peng and M. Mansuripur, Appl. Opt. **43**, 4367 (2004).
[10] N. I. Koroteev, S. A. Krikunov, S. A. Magnitskii, D. V. Malakhov, and V. V. Shubin, Jpn. J. Appl. Phys., Part 1 **37**, 22791 (1998).
[11] X. Jiang, C. Zhou, and F. Gan, Proc. SPIE **4085**, 216 (2001).
[12] T. Ohta, M. Birukawa, N. Yamada, and K. Hirao, J. Magn. Magn. Mater. **242–245**, 108 (2002).
[13] S. M. Wiggins, J. Solis, and C. N. Afonso, Appl. Phys. Lett. **84**, 4445 (2004).
[14] G. Zhang, D. Gu, X. Jiang, Q. Chen, and F. Gan, Solid State Commun. **133**, 209 (2005).
[15] P. L. Liu, R. Yen, and N. Bloembergen, Appl. Phys. Lett. **34**, 864 (1979).
[16] C. V. Shank, R. Yen, and C. Hirlimann, Phys. Rev. Lett. **50**, 454 (1983).
[17] S. K. Sundaram and E. Mazur, Nat. Mater. **1**, 217 (2002).
[18] D. von der Linde, K. Sokolowski-Tinten, and J. Bialkowski, Appl. Surf. Sci. **109/110**, 1 (1997).
[19] J. Siegel, C. N. Afonso, and J. Solis, Appl. Phys. Lett. **75**, 3102 (1999).
[20] S. R. Stiffler, M. O. Thompson, and P. S. Peercy, Phys. Rev. B **43**, 9851 (1991).
[21] P. M. W. French, Rep. Prog. Phys. **58**, 169 (1995).
[22] J. Solis, J. Siegel, and C. N. Afonso, Rev. Sci. Instrum. **71**, 1595 (2000).
[23] J. Bonse, S. M. Wiggins, and J. Solis, Appl. Phys. A **80**, 243 (2005).
[24] M. C. Downer, C. V. Shank, and R. L. Fork, J. Opt. Soc. Am. B **2**, 595 (1985).
[25] J. P. Callan, A. M. -T. Kim, C. A. D. Roeser, E. Mazur, J. Solis, J. Siegel, C. N. Afonso, and J. C. G. de Sande, Phys. Rev. Lett. **86**, 3650 (2001).
[26] C. A. D. Roeser, A. M. -T. Kim, J. P. Callan, L. Huang, E. N. Glezer, Y. Siegal, and E. Mazur, Rev. Sci. Instrum. **74**, 3413 (2003).
[27] S. R. Stiffler, M. O. Thompson, and P. S. Peercy, Phys. Rev. Lett. **60**, 2519 (1988).
[28] K. Sokolowski-Tinten, J. Solis, J. Bialkowski, J. Siegel, C. N. Afonso, and D. von der Linde, Phys. Rev. Lett. **81**, 3679 (1998).
[29] J. Boneberg, O. Yavas, B. Mierswa, and P. Leiderer, Phys. Status Solidi B **174**, 295 (1992).
[30] K. Sokolowski-Tinten, J. Bialkowski, M. Boing, A. Cavalleri, and D. von der Linde, Phys. Rev. B **58**, R11805 (1998).
[31] J. Solis, C. N. Afonso, S. C. W. Hyde, N. P. Barry, and P. M. W. French, Phys. Rev. Lett. **76**, 2519 (1996).